

Gene cluster activation in a bacterial symbiont leads to halogenated angucyclic maduralactomycins and spirocyclic actinospirols

Huijuan Guo,^{*a} Jan W. Schwitalla,^a Rene Benndorf,^a Martin Baunach,^b Christoph Steinbeck,^c Helmar Görls,^d Z. Wilhelm de Beer,^e Lars Regestein^a and Christine Beemelmans^{*a}

a. Leibniz Institute for Natural Product Research and Infection Biology – Hans Knöll Institute (HKI), Beutenbergstraße 11a, 07745 Jena, Germany, E-mail: Huijuan.Guo@hki-jena.de; Christine.Beemelmans@hki-jena.de

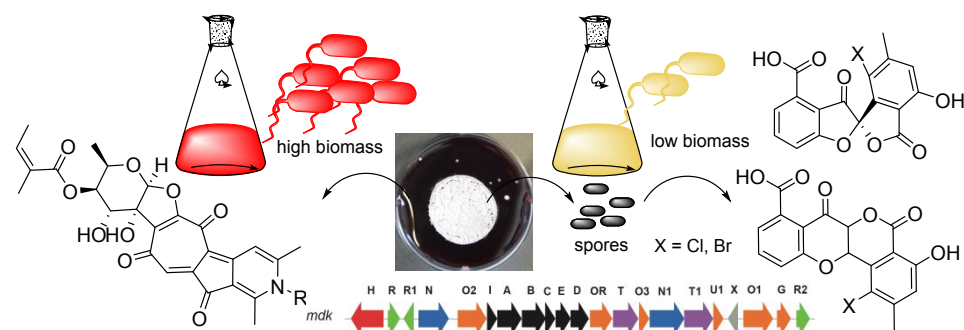
b. University of Potsdam, Institute for Biochemistry and Biology, Karl-Liebknecht Str. 24-25, 14476, Potsdam, Germany

c. Department of Cheminformatics and Computational Metabolomics, Friedrich-Schiller-University, Lessingstr. 8, 07743, Jena, Germany

d. Institute for Inorganic and Analytical Chemistry, Friedrich-Schiller-University, Lessingstr. 8, 07743, Jena, Germany

e. Department of Biochemistry, Genetics and Microbiology, Forestry and Agricultural Biotechnology Institute (FABI), University of Pretoria, Hatfield, 0002, Pretoria, South Africa

Electronic Supplementary Information (ESI) available: culture conditions, isolation procedures, activity assays, ESI-HRMS, NMR spectra of compounds **1-4** and crystallographic data are described within the Supporting Information



ABSTRACT: Growth from spores activated a biosynthetic gene cluster in *Actinomadura* sp. RB29 resulting in the identification of two novel groups of halogenated polyketide natural products, named maduralactomycins and actinospirols. The unique tetracyclic and spirocyclic structures were assigned based on a combination of NMR analysis, chemoinformatic calculations, X-ray crystallography and ¹³C-labeling studies. Based on HRMS²-data, genome mining and gene expression studies we propose an underlying non-canonical angucycline biosynthesis and extensive post-PKS oxidative modifications.

Microbial symbionts, in particular Actinomycetes, have long been recognised as important sources for potent bioactive molecular scaffolds with a broad array of biological activities.¹ Despite decade long research, only global genome sequencing efforts and comparative bioinformatics studies revealed their true untapped biosynthetic potential.² Converting the genetic “blueprints”, however, into purified molecules still remains a significant scientific challenge. Although a plethora of molecular and microbial methods have been used to elicit the transcription of downregulated or silenced gene cluster, the application of ecological-based stress factors, such as microbial challenging assays, have been amongst the most effective triggers and resulted in the isolation of many new natural products with remarkable bioactivities.³⁻⁷

In light of our previous ecology-guided natural product discovery efforts,⁸ we studied the bacterial symbiont of fungus-growing termites, named *Actinomadura* sp. RB29 (5-2),⁹ which exhibited strong antagonistic effect against parasitic

co-isolated fungi of *Macrotermes natalensis*. Intensive chemical analyses led to the isolation of antifungal lanthipeptide rubrominins and polyketide-derived rubterolones.⁹⁻¹¹ Following up on these initial studies, we investigated RB29 cultures when growth was initiated from spores under diluted conditions to simulate the reduced cell densities that the bacterial strains are expected to face under the natural ecological environment when entering the fungus-comb via the obligatory insect gut passage of a termite worker. Detailed LC-MS based analysis of resulting culture extracts indicated a metabolomics shift towards the production of yet unidentified mono-chlorinated metabolites with pseudomolecular ion peaks at *m/z* 360.9 and 374.9, respectively and dereplication of HRMS values using Antibase and Scifinder indicated that both signals might represent yet unreported metabolites.¹² Here, we report on the activation of a cryptic gene cluster based on an ecology-guided cultivation

approach that led to the isolation of four so far unreported tetracyclic secondary metabolites.

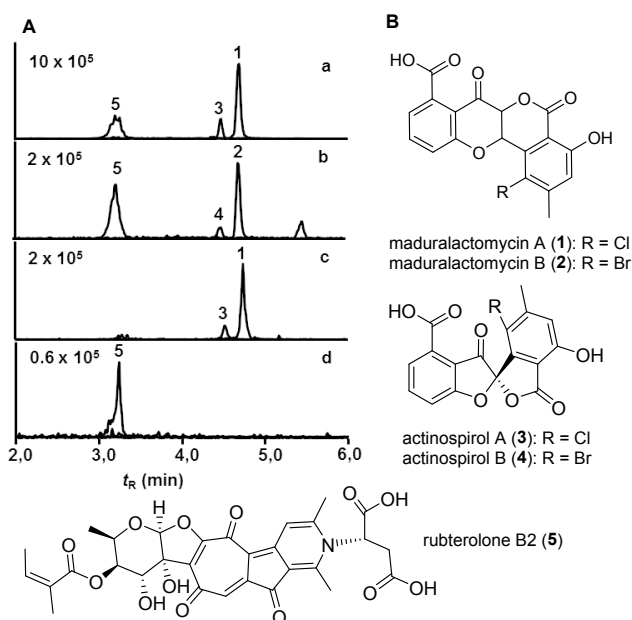


Figure 1. A) UHPLC-MS chromatogram of crude extract under extracted ion chromatogram (EIC+) mode derived from: a) 20 L culture broth + 0.1% NaCl, spore inoculum; b) 20 L culture broth + 0.1% KBr, spore inoculum; c) 100 mL culture broth + 0.1% NaCl, spore inoculum; d) 100 mL culture broth + 0.1% NaCl, vegetative cell inoculum (1: m/z 374.9; 2: m/z 418.9; 3: m/z 360.9; 4: m/z 404.9; 5: rubterolone B2 (m/z 612.1)); B) structures of maduralactomycins A and B, actinospirols A and B and the abundant rubterolone B2.

To analyse the metabolome more in detail, we cultivated RB29 from small to pilot scale (100 mL to 30 L) by starting either from spore solutions or bacterial biomass (stationary phase). Comparative UHPLC-MS analysis revealed that only cultures initiated from spore solutions (either stirring or shaking) were characterized by lower biomass production and low titres of rubterolones, but notable production levels of chlorinated target molecules in a ratio of approx. 1:4 of compound 3 and 1 (Figure 1a, based on peak area of m/z 360.9:374.9 under EIC+ mode). Using cultivation conditions that contained additional NaCl (0.1% – 0.5%, in ISP5* medium) significantly increased production levels of both target compounds. Exchange of NaCl by KBr resulted in the formation of both brominated analogues in a similar ratio (1:4, m/z 404.9 and 418.9 under EIC+ mode) indicating that the underlying biosynthetic enzyme readily accepts both halogen sources, with chloride being likely the most dominant source in the natural environment

For structural elucidation, RB29 was then cultivated in a 30 L stirred tank reactor (6 d, 30 °C) using spore inoculum. Metabolites were extracted using XAD16 resin-based solid phase extraction and subsequent purification was performed by reverse-phase C18 SPE cartridges and MS-guided semi-preparative chromatographic purification, which finally resulted in the isolation of analytically-pure chlorinated and brominated compounds 1 – 4.

The molecular formula of the major chlorinated metabolite 1 was assigned as C₁₈H₁₁O₇Cl by high resolution

mass (HRMS) analysis (ESI) m/z 375.0265 ($[M+H]^+$ $\Delta = -0.23$ ppm) and chlorine-type isotopic pattern.

Detailed 1D/2D NMR analysis (¹H NMR, COSY; HSQC and HMBC) indicated the presence of one methyl group, four aromatic protons, one methine and one carbonyl unit. COSY and HMBC correlations of three aromatic protons (H-3, H-4 and H-5) suggested that they are located on a three-fold substituted aromatic ring D (Figure 2). The fourth singlet aromatic proton indicated towards a five-fold substituted second aromatic moiety (ring A) with diagnostic chemical shifts at δ_C 111.7 ppm and 144.3 ppm, which carried the chlorine substituent and methyl group (C-18), respectively. The characteristic chemical shift of the diagnostic methine proton (H-10, ring B) indicated an oxygen substituent; further HMBC correlations showed that ring B is likely interconnected with ring A and a third ring C carrying the keto/enol moiety (C-8). To verify our structure assumption, we performed ¹³C chemical shift predictions using GIAO density functional theory (DFT) calculations,¹³ which overall supported the assigned 2D structure of 1 (Figure 2, Table S2, S3). However, any attempt to determine the absolute structure by x-ray crystallography failed so far. Cultivation experiments using 0.1% KBr as halogen source resulted in the isolation of a homolog compound 2 assigned as C₁₈H₁₁O₇Br (m/z 418.9749 ($[M+H]^+$ $\Delta = -2.89$ ppm). Comparison of chemical shifts between 1 and 2 revealed a highly similar NMR pattern, except the high-field shift of ¹³C resonance attached to the bromine atom (δ_{C-16} : 111.7 ppm for 1; δ_{C-16} : 100.2 ppm for 2). Overall, compound 1 and 2 exhibited a very rare chromonoisocoumarin fused core structure with structural similarities to the plant-derived distemonanthin, peltogynol and mopanol.¹⁴ Based on their oxidized and rearranged angucycline-type structure derivatives 1 and 2 were named as maduralactomycins A (1) and B (2), respectively.

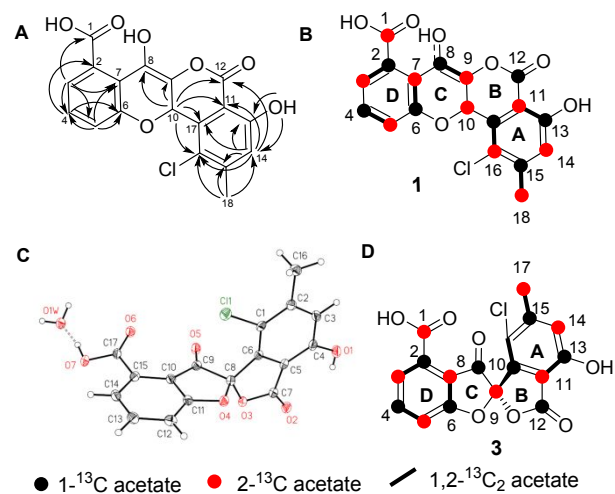


Figure 2. Planar structures of maduralactomycin A (1) showing A) HMBC correlations and B) ¹³C acetate labelling pattern. C) Crystal structure of actinospirol A (3) shown as ORTEP plot with displacement ellipsoids of non-hydrogen atoms drawn at 50% probability level and D) molecular structure and atom labeling of actinospirol A (3) showing ¹³C-acetate labelling pattern.

Our comparative LC-MS analysis further indicated a minor, probably structurally related, chlorinated metabolite 3, which was assigned as C₁₇H₉O₇Cl based on the protonated molecular ion at m/z 361.0105 ($[M+H]^+$ $\Delta = -1.18$ ppm) and a chlorine-typical isotopic pattern. Detailed analysis of ¹H and ¹³C NMR

and HSQC spectra of **3** revealed again the presence of one methyl group and four aromatic protons.

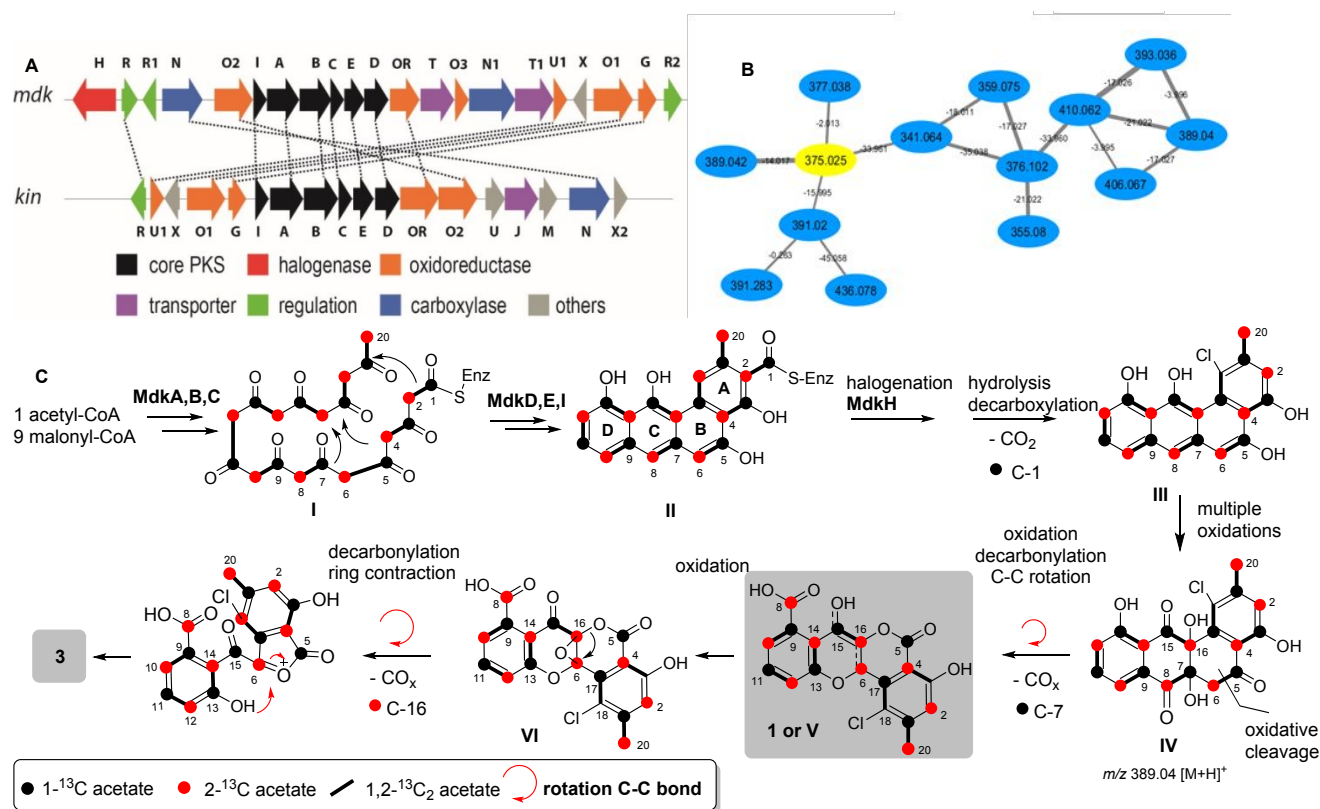


Figure 3. A) Comparison of *mdk* gene cluster (maduralactomycins) and *kin* gene cluster (kanamycin). B) GNPS-based molecular network centred on compound **1** (yellow label). Nodes (circles) represent chemical features. Internal node labels display the precursor mass of compounds (m/z [M+H]⁺). Line widths of edges mirror cosine distances. C) Biosynthetic proposal for the formation of compound **1** and **3** based on gene cluster homologies, GNPS molecular network analysis and ¹³C-labeling studies (here: atom numbering according to biosynthetic origin).

However, the diagnostic methine proton was missing. COSY correlations of H-3, H-4 and H-5 suggested that three aromatic protons are located on the same aromatic ring and HMBC correlations confirmed similar D-ring connections as for maduralactomycin A (**1**). Again, one isolated aromatic proton, the connecting HMBC correlations and the chlorination pattern indicated the same five-fold substitution pattern of a second aromatic moiety. As other diagnostic HMBC correlations were not detectable, we performed again *in silico* ¹³C chemical shift calculations of possible structural isomers using Gaussian 16, which clearly supported our structural assignment (Figure 1, Table S4). Finally, the absolute structure was unambiguously solved by single X-ray analysis from a single crystal prepared in MeOH and H₂O mixture by slow evaporation, and data were collected on a Nonius KappaCCD diffractometer using graphite-monochromated Mo-K α radiation (Figure 2). Based on its microbial origin and its spirocyclic structure, we named the new compound actinospirol A (**3**). The structure of brominated analogue **4** (actinospirol B) was elucidated based on the high-resolution molecular ion signal at m/z 404.9598 ([M+H]⁺ Δ = - 1.56 ppm, C₁₇H₉O₇Br), the diagnostic bromine isotopic pattern and a detailed comparative 2D NMR analysis.

While maduralactomycins (**1**, **2**) resemble in part kinamycin-type compounds,¹⁵ such as dehydrabelomycin,

kinobscurinone, and stealthin C,¹⁶ actinospirols (**3**, **4**) feature a highly intriguing five-membered spiroketal moiety similar to the core moiety of rubromycin polyketides and the antibacterial natural product armeniaspirols derived from *Streptomyces* and pseurotin A from *Aspergillus*.^{17,18} As both compound **1** and **3** share similar structural elements, we hypothesized that both share the same biosynthetic origin, but might have undergone different levels of oxidative post-PKS modifications such as C-H bond oxidation and/or Baeyer-Villiger-type of oxidative rearrangements.

Thus, we performed ¹³C labelling studies. As shown in Figure 2, the observed 1-¹³C, 2-¹³C and 1,2-¹³C₂ acetate labelling pattern and ¹³C coupling constants (1,2-¹³C₂ acetate) confirmed the type-II-PKS origin of both compound classes and highlighted the complex oxidative rearrangement of the core structures. In particular 1,2-¹³C₂ acetate labelling experiments resulted in the isolation of compound **1c**, which carries two singlet carbon atoms at position C-10 and C-12 originally derived from two different acetate units (Figure 2, S3). Similarly, **3c** contains two singlet carbon atoms at position C-8 and C-9 that was previously not directly connected (Figure 2, Figure S4).

We then analysed the genome of RB29 for a putative type II PKS gene cluster using AntiSMASH,¹⁹ MiBIG²⁰ and BLASTp²¹ and found only one type II PKS gene cluster (*mdk*, approx. size: 36 kbp) region that encoded for about 21 genes

including the necessary oxidative enzymes and a halogenase (Figure 3A, Table S5), which showed high similarities, and in part identical gene organization, to the known kinamycin (*kin*) cluster from *Streptomyces murayamaensis*²² and also moderate to high similarities to genes involved in the biosynthesis of jadomycin (*jad*),²³ landomycin (*lan*),²⁴ and simocyclinone (*sim*).²⁵ Interestingly, core genes of the *mdk* cluster are flanked by at least three regulatory genes (MdkR, MdkR1, and MdkR2) including a putative TetR/AcrR transcriptional regulators (MdkR)^{26,27} that are suspected to control gene expression and gene cluster cross-talk, similar as reported for the kinamycin biosynthesis.^{15,28,29} Subsequent RT-PCR analysis of selected key genes of *mdk* verified that the BGC region *mdk* is only transcribed when RB29 culture was started from spores in ISP5* and silenced when cultivation was performed in ISP2 using vegetative mycelium (Figure S10). We also tested if the rubterolones influences the production of **1-4** and found that addition of rubterolones to spore-induced cultures caused a weak upregulation of compounds **1** and **3** (Figure S3), indicating that this compound class is activating, but not repressing the *mdk* transcription.

Additionally, we performed MS²-based mass spectral mediated molecular networking (GNPS) analysis using enriched culture extracts,³⁰ which allowed us to trace back a MS²-cluster corresponding to compound **3** and related (non-chlorinated) derivatives and putative biosynthetic intermediates supporting the overall proposed biosynthesis (*vide infra*, Figure 3B, Table S5-6) and indicating that enzymatic chlorination might be less effective than originally anticipated. In contrast, for compound **1** and rubterolones only single nodes were detectable.

The collected data allowed us then to propose a first biosynthetic pathway for compound **1** and **3** (Figure 3C). The biosynthesis presumably starts with the loading of an acetate unit onto the acyl carrier protein (ACP, MdkC), which then is extended by the ketosynthase (KS, MdkA) and chain-length factor (CLF domain, MdkB) using malonyl CoA yielding the β -keto chain (**I**).³¹ Subsequent cyclization and aromatization of the β -keto chain by the combined action of two different cyclases (MdkD, MdkI) and an aromatase (MdkE) results in the formation of putative intermediate **II**. Although details of the cyclization mechanism are currently unclear, the observed ¹³C labelling pattern for both compounds (**1** and **3**) points towards an unprecedented cyclization mode that appears to be different from the canonical angucycline biosynthesis.^{31,32} Subsequent halogenation (MdkH, Flavin-dependent halogenase, 67% identities with HalB) and decarboxylation of C-1 (atom numbering according to biosynthetic origin) presumably result in an intermediate **III** or a related derivative. Here, it is important to note that compounds **1-4** are halogenated only once at a sterically hindered position (C-18) indicating towards either the intermediate presence of a C1-carboxyl group that blocks the more reactive phenolic *ortho*-position (C-2) and/or a highly regioselective halogenase.³³ In a next step, intermediate **III** (or a related) presumably undergoes extensive (multi-step) post-PKS oxidative rearrangements yielding first an intermediate of type **IV** and/or compound **1**, which after decarboxylation of C-7 results in the formation of the chromen-4-one-containing compound **1**. Subsequent oxidative spirocyclization catalysed again by one of the encoded oxygenases presumably forms **3**. To classify the encoded oxygenases we performed a detailed phylogenetic analysis of key genes encoded within *mdk* (Figure S7 and

Table S4), which suggested that oxidative rearrangements towards compound **1** and **3** likely occurs in a similar fashion as proposed for the kinamycin biosynthesis. In particular, MdkG showed similarity with AlpJ (58% identities) and KinG (60% identities), which catalyse the B-ring cleavage and contraction in kinamycin.³⁴ In analogy to the proposed griseorhodin biosynthesis, which involves FAD-dependent oxygenases (GrhO5, GrhO6, GrhO8, and GrhO9), the homologous flavoenzymes in *mdk* (MdkOR, MdkOI and MdkO2) might initialize oxidative C-ring cleavage, ring contraction, oxidative removal of C-16 and final spiroketal formation to yield compound **3**.³⁵

The molecular aesthetics and biological activity of natural angucyclins and benzannulated spiroketals has also resulted in significant efforts towards their synthesis. Hence, we evaluated the pharmacological potential of maduralactomycin A (**1**) and actinospirol A (**3**). Although, neither **1** nor **3** showed antiproliferative cytotoxicity and antiviral activity, maduralactomycin A (**1**) exhibited moderate antibacterial activity against VRSA *Enterococcus faecalis* and *Mycobacterium vaccae* (Table S8).

In summary, we have identified four tetracyclic natural products **1-4** by activation of a cryptic gene cluster from the bacterial symbiont *Actinomadura* sp. RB29. Based on comparative genome analysis, HRMS²-based GNPS analysis and RT-PCR studies we propose a putative biosynthetic mechanism including a non-canonical angucycline biosynthesis and extensive oxidative modifications ultimately resulting in the formation of antimicrobial maduralactomycins and spirocyclic actinospirols. Overall, our studies highlight that polyketide biosynthesis may be intertwined with the growth stage of *Actinomadura* sp., which could point to a natural function as intra- or extracellular regulatory molecules.

ASSOCIATED CONTENT

Supporting Information

Supporting Information part I (PDF) contains all information regarding culture conditions, isolation procedures, structure elucidation, activity assays, ESI-HRMS and crystallographic data. Crystallographic data deposited at the Cambridge Crystallographic Data Centre under CCDC-1980924 for **3** contain the supplementary crystallographic data excluding structure factors; this data can be obtained free of charge via www.ccdc.cam.ac.uk/conts/retrieving.html (or from the Cambridge Crystallographic Data Centre, 12, Union Road, Cambridge CB2 1EZ, UK; fax: (+44) 1223-336-033; or deposit@ccdc.cam.ac.uk).

Supporting Information part I (PDF) contains all 1 and 2D NMR spectra of compounds **1-4**.

The Supporting Information is available free of charge on the ACS Publications website.

AUTHOR INFORMATION

Corresponding Author

* Dr. Huijuan Guo: Huijuan.Guo@hki-jena.de;

* Dr. Christine Beemelmans: Christine.Beemelmans@hki-jena.de.

Author Contributions

The manuscript was written through contributions of all authors.

All authors have given approval to the final version of the manuscript.

Notes

Conflict of Interest

There are no conflicts of interest to declare.

ACKNOWLEDGMENT

We are grateful for financial support from the German Research Foundation (DFG, BE 4799/2-1 and 3-1, CRC1127 project A6). We wish to thank Ms. Heike Heinecke (Hans Knöll Institute, Jena) for measurement of NMR spectra, and Michaela Schmidtke (Friedrich-Schiller University of Jena), Ms. Christiane Weigel (Hans Knöll Institute, Jena) and Dr. Hans-Martin Dahse (Hans Knöll Institute, Jena) for first bioactivity studies.

REFERENCES

1. Van Arnem, E. B.; Currie, C. R.; Clardy, J. *Chem. Soc. Rev.* **2018**, *47*, 1638-1651.
2. Adamek, M.; Alanjary, M.; Ziemert, N. *Nat. Prod. Rep.* **2019**, *36*, 1295-1312.
3. Weber, T. *Nat. Prod. Rep.* **2019**, *36*, 1231-1232.
4. Xu, F.; Wu, Y.; Zhang, C.; Davis, K. M.; Moon, K.; Bushin, L. B.; Seyedsayamdost, M. R. *Nat. Chem. Biol.* **2019**, *15*, 161-168.
5. Musiol-Kroll, E. M.; Tocchetti, A.; Sosio M.; Stegmann, E. *Nat. Prod. Rep.* **2019**, *36*, 1351-1369.
6. Netzker, T.; Fischer, J.; Weber, J.; Mattern, D. J.; König, C. C.; Valiante, V.; Schroeckh, V.; Brakhage, A. A. *Front Microbiol.* **2015**, *6*, 299.
7. Ramadhar, T. R.; Beemelmans, C.; Currie, C. R.; Clardy, J. *J. Antibiot. (Tokyo)* **2014**, *67*, 53.
8. Benndorf, R.; Martin, K.; Kufner, M.; de Beer, Z. W.; Vollmers, J.; Kaster, A.-K.; C. Beemelmans, C. *IJSEM manuscript in revision* 2020.
9. Benndorf, R.; Guo, H.; Sommerwerk, E.; Weigel, C.; Garcia-Altares, M.; Martin, K.; Hu, H.; Kuefner, M.; de Beer, Z. W.; Poulsen, M.; Beemelmans, C. *Antibiotics* **2018**, *7*, pii: E83.
10. Guo, H.; Benndorf, R.; Lechnitz, D.; Klassen, J. K.; Vollmers, J.; Görls, H.; Steinacker, M.; Weigel, C.; Dahse, H. M.; Kaster, A. K.; de Beer, Z. W.; Poulsen, M.; Beemelmans, C. *Chem. Eur. J.* **2017**, *23*, 9338-9345.
11. Guo, H.; Benndorf, R.; König, S.; Lechnitz, D.; Weigel, C.; Peschel, G.; Berthel, P.; Kaiser, M.; Steinbeck, C.; Werz, O.; Poulsen, M.; Beemelmans, C. *Chem. Eur. J.* **2018**, *24*, 11319-11324.
12. Laatsch, H. *Antibase Version 5.0 - The Natural Compound Identifier*. Wiley-VCH Verlag GmbH & Co. KGaA, **2017**; <https://sso.cas.org>
13. Buevich, A. V.; Elyashberg, M. E. *Magn. Reson. Chem.* **2017**, *1*, 1-12.
14. Jain, A. C.; Sarpal, P. D.; Seshadri, T. R. *Tetrahedron Lett.* **1966**, *7*, 4381-4386.
15. a) Wang, W.; Li, J.; Li, H.; Fan, K.; Liu, Y. *Biochem. Biophys. Res. Commun.* **2019**, *510*, 601-605; b) Wang, K. A.; Ng, T. L.; Wang, P.; Huang, Z.; Balskus, E. P.; van der Donk, W. A. *Nat. Commun.* **2018**, *9*, 3687; c) Liu, X.; Liu, D.; Xu, M.; Tao, M.; Bai, L.; Deng, Z.; Pfeifer, B. A.; Jiang, M. *J. Nat. Prod.* **2018**, *81*, 72-77.
16. M. K. Kharel, P. Pahari, M. D. Shepherd, N. Tibrewal, S. E. Nybo, K. A. Shaaban and J. Rohr. *Nat. Prod. Rep.* **2012**, *29*, 264-325.
17. Wenke, J.; Anke, H.; Sterner, O. *Biosci. Biotechnol. Biochem.* **1993**, *57*, 961-964.
18. Brimble, M. A.; Stubbing, L. A. in *Synthesis of Saturated Oxygenated Heterocycles I: 5- and 6-Membered Rings*, ed. J. Cossy, Springer, **2014**, pp. 189-267.
19. Blin, K.; Shaw, S.; Steinke, K.; Villebro, R.; Ziemert, N.; Lee, S. Y.; Medema, M. H.; Weber, T. *Nucleic Acid Res.* **2019**, *47*, W81-W87.
20. Kautsar, S. A.; Blin, K.; Shaw, S.; Navarro-Muñoz, J. C.; Terlouw, B. R.; van der Hoof, J. J. J.; van Santen, J. A.; Tracanna, V.; Duran, H. G. S.; Andreu, V. O.; Selem-Mojica, N.; Alanjary, M.; Robinson, S. L.; Lund, G.; Epstein, S. C.; Sisto, A. C.; Charkoudian, L. K.; Collemare, J.; Linington, R. G.; Weber, T.; Medema, M. H. *Nucleic Acids Res.* **2020**, *48*, D454-D458.
21. <https://blast.ncbi.nlm.nih.gov>
22. a) Ito, S.; Matsuya, T.; Omura, S.; Otani, M.; Nakagawa, A. *J. Antibiot.*, **1970**, *23*, 315-317; Gould, S. J. *Chem. Rev.* **1997**, *97*, 2499-2510; b) Gould, S. J.; Hong, S. T.; Carney, J. R. *J. Antibiot. (Tokyo)*. **1998**, *51*, 50-57.
23. Sharif, E. U.; O'Doherty, G. A. *Eur. J. Org. Chem.* **2012**, *11*, 2095-2108.
24. Yushchuk, O.; Kharel, M.; Ostash, I.; Ostash, B. *Appl. Microbiol. Biotechnol.* **2019**, *103*, 1659-1665.
25. Trefzer, A.; Pelzer, S.; Schimana, J.; Stockert, S.; Bihlmaier, C.; Fiedler, H.-P.; Welzel, K.; Vente, A.; Bechthold, A. *Antimicrob. Agents Chemother.* **2002**, *46*, 1174-1182.
26. Deng, W.; Li, C.; Xie, J. *Cell Signal.* **2013**, *25*, 1608-1613.
27. van der Heul, H. U.; Bilyk, B. L.; McDowall, K. J.; Seipke, R. F.; van Wezel, G. P. *Nat. Prod. Rep.* **2018**, *35*, 575-604.
28. Romero-Rodríguez, A.; Robledo-Casados, I.; Sánchez, S. *Biochimica et Biophysica Acta* **2015**, *1849*, 1017-1039.
29. Bunet, R.; Song, L.; Mendes, M. V.; Corre, C.; Hotel, L.; Rouhier, N.; Framboisier, X.; Leblond, P.; Challis, G. L.; Aigle, B. *J. Bacteriol.* **2011**, *193*, 1142-1153.
30. Wang, M.; Carver, J. J.; Phelan, V. V.; Sanchez, L. M.; Garg, N.; Peng, Y.; Nguyen, D. V.; Watrous, J.; Kapono, C. A.; Luzzatto-Knaan, T.; Porto, C.; Bouslimani, A.; Melnik, A. V.; Meehan, M. J.; Liu, W.-T.; Crusemann, M.; Boudreau, P. D.; Esquenazi, E.; Sandoval-Calderón, M.; Kersten, R. D.; Pace, L. A.; Quinn, R. A.; Duncan, K. R.; Hsu, C.-C.; Floros, D. J.; Gavilan, R. G.; Kleigrew, K.; Northen, T.; Dutton, R. J.; Parrot, D.; Carlson, E. E.; Aigle, B.; Michelsen, C. F.; Jelsbak, L.; Sohlenkamp, C.; Pevzner, P.; Edlund, A.; McLean, J.; Piel, J.; Murphy, B. T.; Gerwick, L.; Liaw, C.-C.; Yang, Y.-L.; Humpf, H.-U.; Maansson, M.; Keyzers, R. A.; Sims, A. C.; Johnson, A. R.; Sidebottom, A. M.; Sedio, B. E.; Klitgaard, A.; Larson, C. B.; Boya P, C. A.; Torres-Mendoza, D.; Gonzalez, D. J.; Silva, D. B.; Marques, L. M.; Demarque, D. P.; Pociute, E.; O'Neill, E. C.; Briand, E.; Helfrich, E. J. N.; Granatosky, E. A.; Glukhov, E.; Ryyffel, F.; Houson, H.; Mohimani, H.; Kharbush, J. J.; Zeng, Y.; Vorholt, J. A.; Kurita, K. L.; Charusanti, P.; McPhail, K. L.; Nielsen, K. F.; Vuong, L.; Elfeki, M.; Traxler, M. F.; Engene, N.; Koyama, N.; Vining, O. B.; Baric, R.; Silva, R. R.; Mascuch, S. J.; Tomasi, S.; Jenkins, S.; Macherla, V.; Hoffman, T.; Agarwal, V.; Williams, P. G.; Dai, J.; Neupane, R.; Gurr, J.; Rodríguez, A. M. C.; Lamsa, A.; Zhang, C.; Dorrestein, K.; Duggan, B. M.; Almaliti, J.; Allard, P.-M.; Phapale, P.; Nothias, L.-F.; Alexandrov, T.; Litaudon, M.; Wolfender, J.-L.; Kyle, J. E.; Metz, T. O.; Peryea, T.; Nguyen, D.-T.; VanLeer, D.; Shinn, P.; Jadhav, A.; Müller, R.; Waters, K. M.; Shi, W.; Liu, X.; Zhang, L.; Knight, R.; Jensen, P. R.; Palsson, B. Ø.; Pogliano, K.; Linington, R. G.; Gutiérrez, M.; Lopes, N. P.; Gerwick, W. H.; Moore, B. S.; Dorrestein, P. C.; Bandeira, N. *Nat. Biotechnol.* **2016**, *34*, 828-837.
31. Hertweck, C. *Angew. Chem. Int. Ed.* **2009**, *48*, 4688-4716.
32. Zhou, H.; Li, Y.; Tang, T. *Nat. Prod. Rep.* **2010**, *27*, 839-868.

33. Agarwal, V.; Miles, Z. D.; Winter, J. M.; Eustáquio, A. S.; El Gamal, A. A.; Moore, B. S. *Chem. Rev.* **2017**, *8*, 5618-5674.
34. Wang, B.; Ren, J.; Li, L.; Guo, F.; Pan, G.; Ai, G.; Aigle, B.; Fan, K.; Yang, K. *Chem. Commun.* **2015**, *51*, 8845-8848.
35. Yunt, Z.; Reinhardt, K.; Li, A.; Engeser, M.; Dahse, H. M.; Gütschow, M.; Bruhn, T.; Bringmann, G.; Piel, J. J. *Am. Chem. Soc.* **2009**, *131*, 2297-2305.